Inorganic Chemistry

Article

pubs.acs.org/IC

Metallophilic Contacts in 2-$C_6F_4PPh_2$ Bridged Heterobinuclear Complexes: A Crystallographic and Computational Study

Erik Wächtler,[†,‡] Steven H. Privér,[†] Jörg Wagler,[‡] Thomas Heine,[§] Lyuben Zhechkov,[§] Martin A. Bennett,[∥] and Suresh K. Bhargava*[,†]

[†]Centre for Advanced Materials and Industrial Chemistry (CAMIC), School of Applied Sciences (Applied Chemistry), RMIT University, GPO Box 2476 V, Melbourne, Victoria 3001, Australia

[‡]Institut für Anorganische Chemie, Technische Universität Bergakademie Freiberg, 09596 Freiberg, Germany

[§]Centre for Functional Nanomaterials (Nanofun), Engineering and Science, Jacobs University, 28759 Bremen, Germany

[∥]Research School of Chemistry, Australian National University, Canberra, Australian Capital Territory 2601, Australia

Supporting Information

ABSTRACT: Treatment of the bis(chelate) complex *trans*-[Pd(κ^2-2-$C_6F_4PPh_2$)$_2$] (**7**) with PMe_3 gave *trans*-[Pd(κC-2-$C_6F_4PPh_2$)$_2$(PMe_3)$_2$] (**13**) as a mixture of *syn*- and *anti*-isomers. Reaction of **13** with CuCl, AgCl, or [AuCl(tht)] (tht = tetrahydrothiophene) gave the heterobinuclear complexes [(Me_3P)$_2$Pd(μ-2-$C_6F_4PPh_2$)$_2$MCl] [M = Cu (**14**), Ag (**15**), Au (**16**)], from which the corresponding salts [(Me_3P)$_2$Pd(μ-2-$C_6F_4PPh_2$)$_2$M]PF_6 [M = Cu (**17**), Ag (**18**), Au (**19**)] could be prepared by abstraction of the chloro ligand with $TlPF_6$; **18**, as well as its triflato (**20**) and trifluoroacetato (**21**) analogues, were also prepared directly from **13** and the appropriate silver salt. Reaction of **13** with [AuCl(PMe_3)] gave the zwitterionic complex [(Me_3P)PdCl(μ-2-$C_6F_4PPh_2$)$_2$Au] (**24**) in which the 2-$C_6F_4PPh_2$ ligands are in a head-to-head arrangement. In contrast, the analogous reaction with [AuCl(PPh_3)] gave [(Ph_3P)PdCl(μ-2-$C_6F_4PPh_2$)$_2$Au] (**25**) with a head-to-tail ligand arrangement. Single crystal X-ray diffraction studies of complexes **14**–**21** show short metal–metal separations [2.7707(11)–2.9423(3) Å] suggestive of attractive noncovalent (dispersion) interactions, a conclusion that is supported by theoretical calculations of the electron localization function and the noncovalent interactions descriptor.

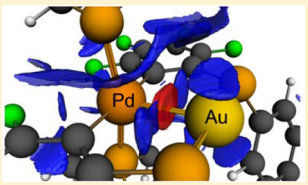

INTRODUCTION

Homobinuclear and heterobinuclear complexes derived from d^8 and d^{10} transition elements have attracted much experimental and theoretical attention because of their intriguing spectroscopic and photophysical properties.[1−8] Many of the binuclear systems based on d^8–d^8 and d^8–d^{10} pairs of metal atoms employ symmetrical bridging ditertiary phosphines, in particular, bis(diphenylphosphino)methane, $Ph_2PCH_2PPh_2$ (dppm), and close relatives such as bis(dicyclohexylphosphino)methane, $Cy_2PCH_2PCy_2$ (dcpm).[9,10]

Shaw et al. first developed systematic procedures for the synthesis of μ-dppm complexes containing d^8 and d^{10} transition elements based on the facile opening of the chelate four-membered ring of suitable P,P′-dppm precursors. For example, [Ir(CO)(P,P′-dppm)$_2$]Cl reacts with [AuCl(PPh_3)] to give the heterobinuclear cationic μ-dppm species **1**, and with CuCl or [AgCl(PPh_3)]$_4$ to give neutral chloro-coordinated heterobinuclear μ-dppm species **2a** and **2b** (Scheme 1).[11,12] Similarly, bis(acetylides) and dicyanides of the type *trans*-[MX_2(κP-dppm)$_2$] (M = Pd, Pt; X = CN, C_2R), which are derived from [M(P,P′-dppm)$_2$]$^{2+}$, form 1:1 adducts on reaction with [AuCl(PPh_3)], $AgNO_3$/KI, or AgOTf (Scheme 2).[13−15] Dicyano-nickel(II), -palladium(II), and -platinum(II) adducts with gold(I) containing μ-dcpm have also been prepared.[1]

Laguna et al. have used the unsymmetrical ligand Ph_2PCH_2SPh to form heterobimetallic Au–Ag and Au–Pd complexes such as **5** (Figure 1), starting from the P-coordinated precursors [Au(κP-Ph_2PCH_2SPh)$_2$]OTf and [AuCl(κP-Ph_2PCH_2SPh)].[16,17]

Single-crystal X-ray structural analyses indicate that the metal atoms in these d^8–d^{10} complexes are in close contact, with separations of ca. 2.9–3.0 Å,[1,12,15−19] and theoretical calculations[1,2,15−19] support the existence of a weak attractive interaction, arising mainly from dispersion forces, reinforced, in

Scheme 1

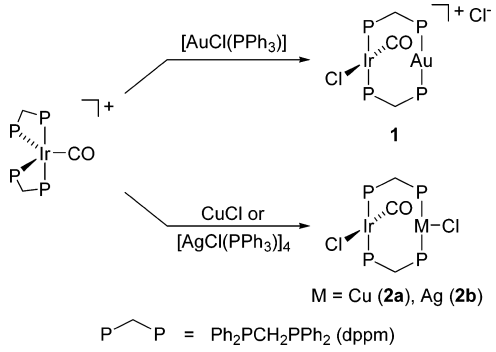

Received: April 27, 2015
Published: June 29, 2015

DOI: 10.1021/acs.inorgchem.5b00939
Inorg. Chem. 2015, 54, 6947−6957

Scheme 2

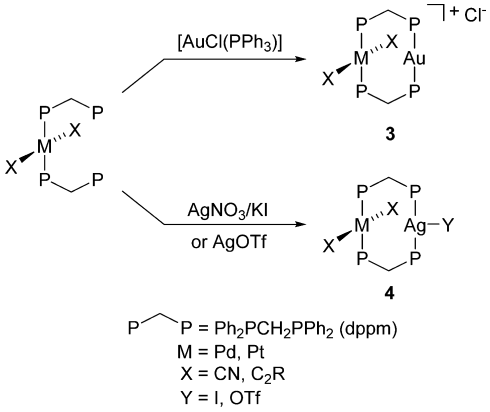

the case of gold, by a relativistic effect, which is responsible for the observed UV-spectroscopic and photophysical properties.

We have been interested in *ortho*-metalated complexes of d^8 and d^{10} transition elements containing carbanionic ligands of the type 2-$C_6R_4PPh_2$ (R = H, F), whose coordination behavior shows some similarity to that of dppm. For example, the divalent d^8 metal bis(chelate) complexes **6** and **7** contain four-membered rings that can be opened by various ligands to give κC-bonded species,[20,21] whereas the binuclear d^9–d^9 diplatinum(I) (**8**)[22] and dipalladium(I) (**9**)[23] complexes, and the binuclear d^{10}–d^{10} digold(I) complexes (**10**)[24−26] contain a pair of 2-$C_6R_4PPh_2$ (R = H, F) groups bridging the metal atoms in a head-to-tail (HT) arrangement.

Also, in recent years, a number of complexes of d^{10} elements have been made from so-called σ-acceptor (ambiphilic) ligands in which one or more 2-$C_6H_4PR_2$ (R = Ph, ^{i}Pr) units are attached to a Lewis acidic main group atom such as boron,[27−29] gallium,[30] indium,[31] silicon,[32] tin,[32] antimony,[33] and bismuth;[34,35] examples are shown in Figures 2 and 3. Experimental and theoretical evidence indicates that the d^{10} element in these compounds behaves as a σ-electron pair donor to the main group element.

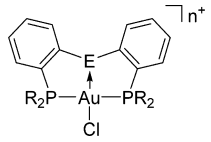

R = Ph, ^{i}Pr; E = BPh; n = 0
R = ^{i}Pr; E = GaCl; n = 0
R = ^{i}Pr; E = PhSiF, PhSnF; n = 0
R = Ph; E = BiCl; n = 0
R = Ph; E = PhSbF, (2-$Ph_2PC_6H_4$)SbF; n = 1

Figure 2.

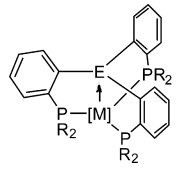

R = ^{i}Pr; E = B; [M] = AuCl, AgCl, CuCl, Pt, Pd, Ni
R = ^{i}Pr; E = In; [M] = Pd
R = ^{i}Pr; E = InCl; [M] = Au
R = Ph; E = SbF; [M] = PdCl

Figure 3.

With this background of the so far investigated d^8–d^{10} heterobimetallic systems with symmetric ligands (which exhibit dispersive metal–metal interactions) and d^{10} → E-systems with ambiphilic ligands (which exhibit Lewis donor–acceptor-interactions), we have investigated the synthesis, molecular structures, and electronic features of the metallophilic interactions of a series of heterobinuclear complexes in which the ambiphilic ligand 2-$C_6F_4PPh_2$ bridges d^8 (Pd^{II}) and d^{10} (Cu^I, Ag^I, Au^I) transition elements. Two examples of d^8–d^{10} complexes of this type are *trans*-[$PdCl_2${(2-$Ph_2PC_6H_4$)$_2$Hg}] (**11**)[36,37] and [{(C_6F_5)$AuCl_2$(2-$Ph_2PC_6H_4$)}$_2$Hg] (**12**),[4] which were prepared from the reaction of [Hg(2-$C_6H_4PPh_2$)$_2$] with [$PdCl_2(SEt_2)_2$] and 2[$AuCl_2(C_6F_5)$(tht)]/$PhICl_2$, respectively; in the case of **12**, theoretical (MP2) calculations indicate the presence of metallophilic (dispersion-type) interactions between the Au^{III} and Hg^{II} atoms.

RESULTS

Treatment of the bis(chelate) complex *trans*-[Pd(κ^2-2-$C_6F_4PPh_2$)$_2$] (**7**) with ca. 3 equiv of PMe_3 cleanly gave the ring-opened product *trans*-[Pd(κC-2-$C_6F_4PPh_2$)$_2$(PMe_3)$_2$] (**13**) in good yields as a mixture of *syn*- and *anti*-isomers (Scheme 3), the structures of which were confirmed by single

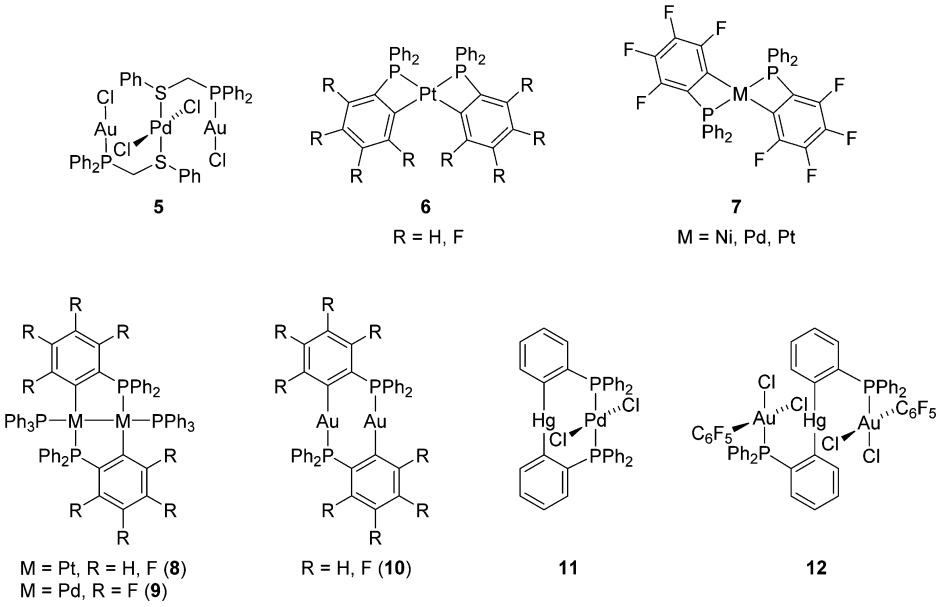

Figure 1.

DOI: 10.1021/acs.inorgchem.5b00939
Inorg. Chem. 2015, 54, 6947−6957

Scheme 3

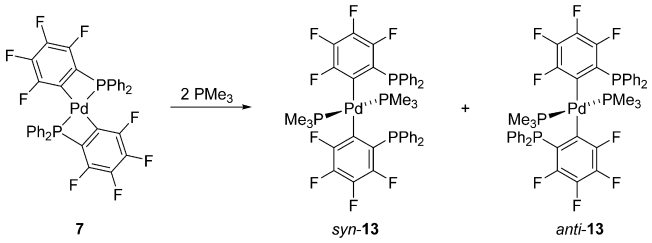

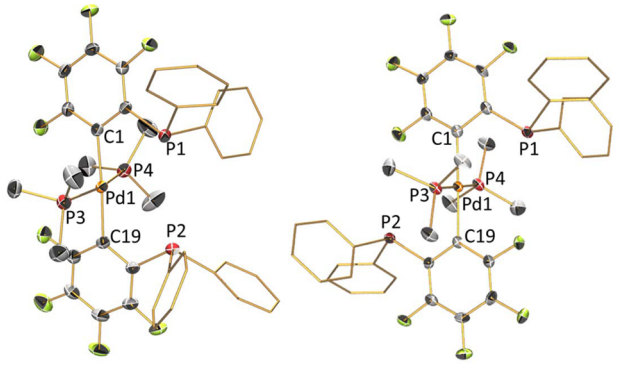

Figure 4. Molecular structures of *syn*- (left) and *anti*- (right) isomers of *trans*-[Pd(κC-2-$C_6F_4PPh_2$)$_2$(PMe_3)$_2$] (**13**). Ellipsoids show 50% probability levels. Hydrogen atoms have been omitted and phenyl groups are depicted as stick models for clarity. Selected bond lengths (Å) and angles (deg): *syn*-**13**: Pd(1)−C(1) 2.0809(15), Pd(1)−C(19) 2.0818(15), Pd(1)−P(3) 2.3118(5), Pd(1)−P(4) 2.2960(5), C(1)−Pd(1)−C(19) 176.02(6), P(3)−Pd(1)−P(4) 166.681(17), C(1)−Pd(1)−P(3) 90.30(4), C(1)−Pd(1)−P(4) 90.34(4), C(19)−Pd(1)−P(3) 88.24(5), C(19)−Pd(1)−P(4) 90.23(4); *anti*-**13**: Pd(1)−C(1) 2.057(7), Pd(1)−C(19) 2.068(7), Pd(1)−P(3) 2.3024(18), Pd(1)−P(4) 2.3085(18), C(1)−Pd(1)−C(19) 179.1(3), P(3)−Pd(1)−P(4) 179.16(8), C(1)−Pd(1)−P(3) 88.65(18), C(1)−Pd(1)−P(4) 90.97(18), C(19)−Pd(1)−P(3) 91.16(18), C(19)−Pd(1)−P(4) 89.44(18).

crystal X-ray diffraction (Figure 4). The reaction of **7** with 2 equiv of PMe_3 gave **13** contaminated with unidentified impurities. Attempts to prepare the PPh_3 analogue of **13** were unsuccessful, and only unreacted starting materials were observed by ^{31}P NMR spectroscopy, even in the presence of a large excess of PPh_3. This failure can probably be ascribed to the poorer σ-donor ability coupled with the greater steric bulk of the triarylphosphine.

The ^{1}H NMR spectrum of **13** showed a single broad resonance at δ 0.47 due to the methyl groups of the PMe_3 ligands, together with the expected aromatic resonances in the region of δ 7.0−7.8. The ^{31}P NMR spectrum showed two pairs of multiplets at δ −2.9 and −19.1, and −8.4 and −18.7, in about a 1:6 ratio, which are assigned to *syn*- and *anti*-isomers; however it is not clear which pair of resonances corresponds to which isomer. In both cases, the more shielded resonance is assigned to the PMe_3 phosphorus nuclei and the deshielded resonance to the uncoordinated PPh_2 group.

In their solid state structures, the *syn*- and *anti*-isomers of *trans*-[Pd(κC-2-$C_6F_4PPh_2$)$_2$(PMe_3)$_2$] (**13**) (Figure 4) exhibit approximately square planar geometry about the metal center and the Pd−P [*syn*-**13**: 2.31, 2.30 Å; *anti*-**13**: 2.30, 2.31 Å] and Pd−C [*syn*-**13**: 2.08, 2.08 Å; *anti*-**13**: 2.06, 2.07 Å] bond lengths are comparable to those in the parent bis(chelate) complex **7** [2.3069(4) and 2.074(4) Å, respectively]. In the *anti*-isomer, the C−Pd−C and P−Pd−P angles are close to perfect linearity [179.1(3) and 179.16(8)°, respectively], while the corresponding angles in the *syn*-isomer are slightly more distorted [176.02(6) and 166.68(2)°, respectively], presumably due to steric effects of the bulky *ortho*-PPh_2 groups.

Reaction of **13** with CuCl, AgCl or [AuCl(tht)] gave the corresponding 1:1 adducts [$(Me_3P)_2Pd(\mu$-2-$C_6F_4PPh_2)_2MCl$] [M = Cu (**14**), Ag (**15**), Au (**16**)] in which the coinage metal atom is coordinated by the two PPh_2 groups (Scheme 4). The ^{31}P NMR spectra of **14**−**16** each showed a pair of multiplet resonances at ca. δ −17 assignable to the coordinated PMe_3 and a second resonance further downfield corresponding to the PPh_2 group (**14**: δ 3.1; **15**: δ 11.8; **16**: δ 37.9). In the case of **15**, the downfield resonance is split into a doublet of multiplets due to coupling with $^{107/109}$Ag (*J* 438 Hz).

Abstraction of the chloride ligand in complexes **14**−**16** with $TlPF_6$ generated the salts [$(Me_3P)_2Pd(\mu$-2-$C_6F_4PPh_2)_2M]PF_6$ [M = Cu (**17**), Ag (**18**), Au (**19**)]. The ^{31}P NMR spectra of **17**−**19** each showed a septet at δ −144.5 and a pair of multiplet resonances, one at ca. δ −15 and the other in the range +11−41, assignable to the phosphorus nuclei in the PF_6^- counterion, PMe_3 ligands, and bridging $C_6F_4PPh_2$ groups, respectively; the downfield shift of the latter increases in the order Cu (δ 11.7) < Ag (δ 18.6) < Au (δ 40.8). The silver complex **18** could also be generated directly from the reaction of *trans*-[Pd(κC-2-$C_6F_4PPh_2$)$_2$(PMe_3)$_2$] (**13**) with $AgPF_6$, although in this case the obtained product was slightly brown, presumably due to traces of silver metal. Reaction of **13** with AgOTf and $AgOOCCF_3$ gave the corresponding cationic complexes in a pure state containing triflate (**20**) and trifluoroacetate (**21**) counterions; as expected, the spectroscopic data for **20** and **21** are comparable to those of **18**.

The molecular structures of the complexes [$(Me_3P)_2Pd(\mu$-2-$C_6F_4PPh_2)_2MCl$] [M = Cu (**14**), Ag (**15**), Au (**16**)] are isomorphous (orthorhombic, space group *Pnma*). As a representative example, the molecular structure of **16** is

Scheme 4

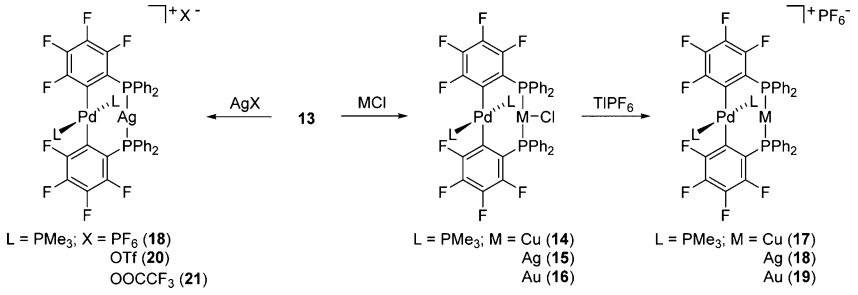

DOI: 10.1021/acs.inorgchem.5b00939
Inorg. Chem. 2015, 54, 6947−6957

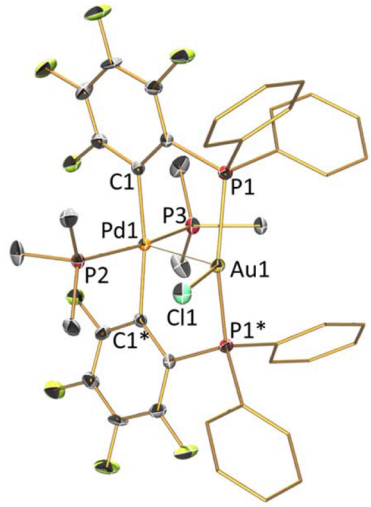

Figure 5. Molecular structure of $[(Me_3P)_2Pd(\mu\text{-}2\text{-}C_6F_4PPh_2)_2AuCl]$ (**16**). Ellipsoids show 50% probability levels. Hydrogen atoms have been omitted and phenyl groups are depicted as stick models for clarity.

Table 1. Selected Bond Lengths (Å) and Angles (deg) in $[(Me_3P)_2Pd(\mu\text{-}2\text{-}C_6F_4PPh_2)_2MCl]$ [M = Cu (14), Ag (15), Au (16)][a]

	14	15	16
Pd(1)···M(1)	2.8448(3)	2.9170(4)	2.8842(4)
Pd(1)−C(1)	2.0652(14)	2.0724(13)	2.062(3)
Pd(1)−P(2)	2.3172(5)	2.3240(6)	2.3207(12)
Pd(1)−P(3)	2.3373(5)	2.3282(6)	2.3270(12)
M(1)−P(1)	2.3071(4)	2.4570(5)	2.3401(9)
M(1)−Cl(1)	2.2843(6)	2.5307(7)	2.6623(12)
P(1)−M(1)−P(1)*	143.42(2)	144.28(2)	152.69(4)
C(1)−Pd(1)−C(1)*	171.31(7)	171.22(8)	172.02(17)
P(2)−Pd(1)−P(3)	167.00(2)	167.47(2)	167.34(4)
C(1)−Pd(1)−P(2)	86.75(4)	86.83(4)	86.56(8)
C(1)−Pd(1)−P(3)	92.51(4)	92.43(4)	92.92(8)

[a]Asterisks indicate symmetry equivalent atoms generated by a crystallographic bisecting plane.

shown in Figure 5, and selected bond lengths and angles for **14**−**16** are collected in Table 1. The palladium atom in **14**−**16** is located in an approximately square planar coordination sphere, and the Pd−P and Pd−C bond lengths are in the expected range for complexes of the type *trans*-$[Pd(PMe_3)_2(aryl)_2]$, for example *trans*-$[(Me_3P)_2Pd\{1\text{-}(n\text{-butyl})tetrazol\text{-}5\text{-}yl\}_2]$ [2.3072(6) and 2.034(3) Å, respectively].[38] Notably, the C−Pd−C (ca. 171°) and P−Pd−P (ca. 167°) angles in **14**−**16** are significantly distorted from linearity, the Pd atom being displaced from the idealized P_2C_2 plane toward the coinage metal. The short Pd···M separations [M = Cu {2.8448(3) Å}, Ag {2.9170(4) Å}, Au {2.8842(4) Å}] are consistent with the presence of weak metallophilic interactions.

Upon replacing the coinage metal-bound chloride in **14**−**16** by the weakly coordinating PF_6^- ion (**17**−**19**), both the head-to-head bridging mode of the bidentate ligands and the *trans*-arrangement of the Pd coordination sphere are retained. In **17** the copper coordination sphere is augmented by a solvent molecule (THF), whereas the silver atom in **18** exhibits a weak contact to one of the PF_6^- fluorine atoms (3.23 Å); the shortest separation between the gold atom in **19** and the counterion is greater than 4 Å. Despite the different degrees of lowering of the coinage metal coordination number, the cationic complexes **17**−**19** exhibit a systematic shortening of their intermetallic separations, by 0.054, 0.049, and 0.087 Å, respectively (see Tables 1 and 2, Figure 6 for the molecular structures of **17** and **19**).

Table 2. Selected Bond Lengths (Å) and Angles (deg) in $[(Me_3P)_2Pd(\mu\text{-}2\text{-}C_6F_4PPh_2)_2M]PF_6$ [M = Cu (17), Ag (18), Au (19)][a]

	17	18	19
Pd(1)···M(1)	2.7707(11)	2.86819(18)	2.7970(4)
Pd(1)−C(1)	2.066(6)	2.0954(14)	2.070(4)
Pd(1)−C(19)	2.057(6)	2.0770(14)	2.080(8)
Pd(1)−P(3)	2.3194(17)	2.3241(4)	2.3172(13)
Pd(1)−P(4)	2.3009(18)	2.3153(4)	2.32*
M(1)−P(1)	2.2173(18)	2.4201(4)	2.3120(12)
M(1)−P(2)	2.2143(18)	2.4265(4)	2.3120(12)
P(1)−M(1)−P(2)	155.39(7)	160.016(13)	169.26(4)
C(1)−Pd(1)−C(19)	177.2(2)	173.97(6)	178.14(17)
P(3)−Pd(1)−P(4)	167.80(6)	167.979(14)	171.5(2)
C(1)−Pd(1)−P(3)	90.35(16)	92.69(4)	88.52(12)
C(1)−Pd(1)−P(4)	89.94(17)	87.45(4)	90.7*
C(19)−Pd(1)−P(3)	90.62(15)	89.89(4)	89.89(13)
C(19)−Pd(1)−P(4)	88.56(16)	88.90(4)	90.7*

[a]Asterisks indicate average values from two different (but similar) bond lengths or angles, which arise from the refinement of $P(4)Me_3$ in two disorder positions.

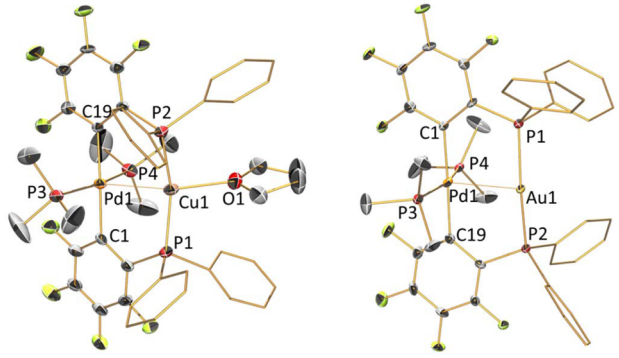

Figure 6. Molecular structures of the cations in $[(Me_3P)_2Pd(\mu\text{-}2\text{-}C_6F_4PPh_2)_2Cu(THF)]PF_6$ (**17**) (left) and $[(Me_3P)_2Pd(\mu\text{-}2\text{-}C_6F_4PPh_2)_2Au]PF_6$ (**19**) (right). Ellipsoids show 50% probability levels. For clarity, hydrogen atoms have been omitted, and phenyl groups are depicted as stick models.

The palladium−silver complexes $[(Me_3P)_2Pd(\mu\text{-}2\text{-}C_6F_4PPh_2)_2Ag]X$ [X = OTf (**20**), $OOCCF_3$ (**21**)] are structurally similar to complex **18** and consist of a pair of metal atoms bridged by two $2\text{-}C_6F_4PPh_2$ ligands in a head-to-head arrangement (Figure 7). The palladium atom is bound by two PMe_3 ligands and two carbon atoms of the bridging ligands and the silver atom by the two phosphorus atoms of the $2\text{-}C_6F_4PPh_2$ groups. The metrical parameters in **18**, **20**, and **21** are generally similar, although the Pd−C and Ag−P bond lengths are slightly longer and shorter, respectively, than those in $[(Me_3P)_2Pd(\mu\text{-}2\text{-}C_6F_4PPh_2)_2AgCl]$ (**15**). In **18** and **20**, the Pd···Ag separation [2.8682(2) and 2.7948(2) Å, respectively] is significantly smaller, and the P−Ag−P angle [160.02(1) and 163.65(2)°, respectively] larger, than those in **15** [2.9170(4) Å,

DOI: 10.1021/acs.inorgchem.5b00939
Inorg. Chem. 2015, 54, 6947−6957

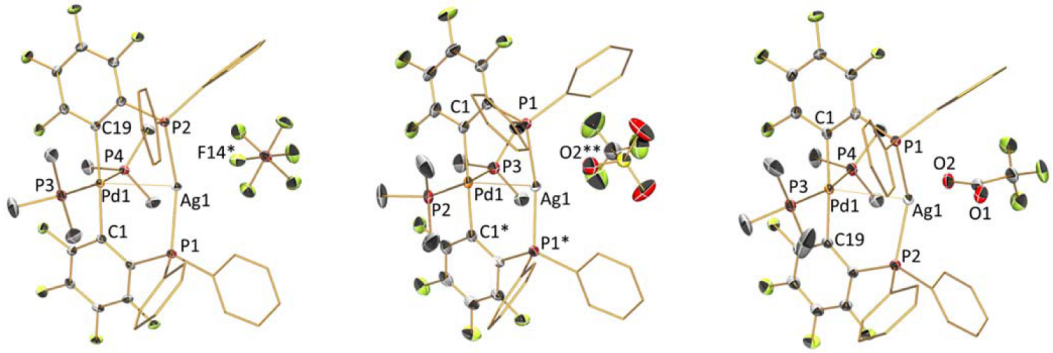

Figure 7. Molecular structures of $[(Me_3P)_2Pd(\mu\text{-}2\text{-}C_6F_4PPh_2)_2Ag]PF_6$ (**18**), $[(Me_3P)_2Pd(\mu\text{-}2\text{-}C_6F_4PPh_2)_2Ag]OTf$ (**20**), and $[(Me_3P)_2Pd(\mu\text{-}2\text{-}C_6F_4PPh_2)_2Ag]OOCCF_3$ (**21**). Ellipsoids show 50% probability levels. For clarity, hydrogen atoms have been omitted, and phenyl groups are depicted as stick models.

144.28(2)°], reflecting the effect the presence or absence of a ligand bound to the silver atom has on the metrical parameters of the complex. In contrast to **18** and **20**, in the trifluoroacetato complex **21**, the counterion is coordinated to the silver atom [Ag−O 2.599(2), 2.517(3) Å], resulting in a Pd···Ag separation [2.9423(3) Å] that is longer than that observed in **15**, **18**, and **20**. The P−Ag−P angle [146.66(3)°] in **21** is also significantly smaller than those in **18** and **20**, but similar to that in **15**; the geometry about the silver atom in **21** is best described as distorted trigonal bipyramidal.

Table 3. Selected Bond Lengths (Å) and Angles (deg) in $[(Me_3P)_2Pd(\mu\text{-}2\text{-}C_6F_4PPh_2)_2Ag]X$ [X = PF_6 (18), OTf (20), $OOCCF_3$ (21)]

	18	20	21[a]
Pd(1)···Ag(1)	2.86819(18)	2.7948(2)	2.9423(3)
Pd(1)−C(1)	2.0954(14)	2.0903(14)	2.079(3)
Pd(1)−C(19)	2.0770(14)		2.093(3)
Pd(1)−P(3)	2.3241(4)	2.3345(6)	2.3205(8)
Pd(1)−P(4)	2.3153(4)		2.3212(8)
Ag(1)−P(1)	2.4201(4)	2.3969(3)	2.4325(8)
Ag(1)−P(2)	2.4265(4)		2.4242(8)
P(1)−Ag(1)−P(2)	160.016(13)	163.650(17)	146.66(3)
C(1)−Pd(1)−C(19)	173.97(6)	176.28(7)	174.88(11)
P(3)−Pd(1)−P(4)	167.979(14)	166.953(19)	165.69(3)
C(1)−Pd(1)−P(3)	92.69(4)	91.19(4)	89.65(8)
C(1)−Pd(1)−P(4)	87.45(4)		87.87(8)
C(19)−Pd(1)−P(3)	89.89(4)	88.52(4)	90.84(7)
C(19)−Pd(1)−P(4)	88.90(4)		90.41(7)

[a]Ag(1)−O(1) 2.599(2), Ag(1)−O(2) 2.517(3).

In compounds **14**−**21** the interatomic separations of the palladium and coinage metal (CM) atom are very close to the sum of their covalent radii[39] (relative separations range between 0.98 and 1.05). In order to shed some light on the interaction between Pd and the CM atom in these complexes we performed natural bond orbital (NBO) and natural localized molecular orbital (NLMO) analyses of the wave functions calculated for their solid state molecular configurations (the atomic coordinates of non-hydrogen atoms were retained; only the positions of the hydrogen atoms were optimized). The analyses could not identify any NLMO for the Pd···CM interaction (NLMOs which are composed of significant contributions of both metal atoms). Instead, we found NLMOs which represent electron lone pairs at the metal atoms (five such NLMOs at CM and four at Pd). Each NLMO which has significant contributions of Pd or CM exhibits less than 0.35% contribution of CM or Pd, respectively, and we interpret this observation as the absence of any significant Pd-CM lone-pair donor−acceptor interaction. In general, they consist of at least 95% metal contribution, whereas other contributions are scattered over various atoms in the ligand sphere, each contribution being less than 1%. Thus, these NLMOs reflect the d^{10} (CM) and d^8 (Pd) configurations of the metal atoms. In addition, for Pd we found two NLMOs which are representative of Pd−C and Pd−P covalent bonding interactions.

A closer investigation of the electron density features along the Pd-CM axis (electron localization function ELF) reveals that there is basically no electron density localization between the two metal atoms (as shown for the Pd−Au complexes **16** and **19** in Figure 8, top). Instead, analysis of the noncovalent

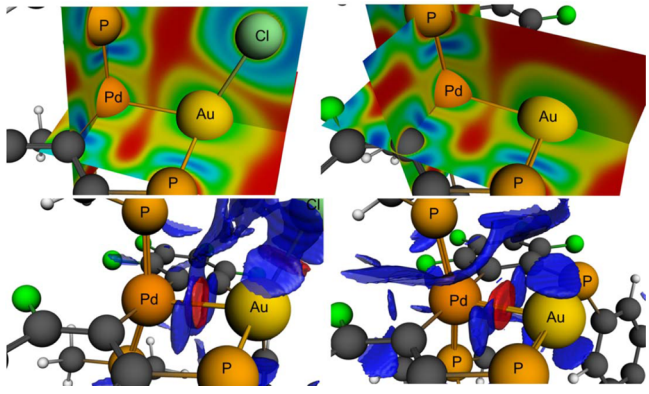

Figure 8. ELF (above) and NCI (below) for compounds **16** (left) and the cation of **19** (right). Color codes for ELF: strong delocalization red; strong localization blue; for NCI: attractive interactions red; nonattractive interactions blue.

interactions descriptor (NCI) of **16** and **19** (Figure 8, bottom) clearly shows that noncovalent attractive forces exist between the metal atoms. This interaction is pronounced for the cationic compound **19** (which is in accord with the shorter Pd−Au separation found in its solid state structure). Apparently, dispersion forces outweigh the Coulomb repulsion between the cationic metal centers.

The natural charges (NCs) of the metal atoms and of their ligand donor atoms are shown in Table 4. The NCs of the Pd

DOI: 10.1021/acs.inorgchem.5b00939
Inorg. Chem. 2015, 54, 6947−6957

Table 4. Selected Natural Charges (NC) of the Pd Atoms, Coinage Metal (CM) Atoms and Their Ligand Donor Atoms As Well as Pd···CM Separations (in Å) and the Ratio *r*(Pd···CM) (Interatomic Separation Divided by the Sum of the Covalent Radii) in Compounds 14−21

	14	17	21	15	18	20	16	19
CM	Cu	Cu	Ag	Ag	Ag	Ag	Au	Au
NC(CM)	0.56	0.54	0.58	0.56	0.48	0.46	0.38	0.21
NC(Pd)	0.27	0.26	0.27	0.27	0.25	0.25	0.28	0.26
NC(Cl_{CM})	−0.76			−0.79			−0.78	
NC(P_{CM})	0.71	0.71	0.70	0.72	0.73	0.73	0.79	0.82
NC(P_{Pd})	0.92	0.92	0.92	0.93	0.92	0.92	0.93	0.93
NC(C_{Pd})	−0.31	−0.30	−0.30	−0.30	−0.31	−0.30	−0.30	−0.30
Pd···CM	2.845	2.771	2.942	2.917	2.868	2.795	2.884	2.797
r(Pd···CM)	1.050	1.022	1.036	1.027	1.010	0.984	1.049	1.017
ΣNC(Pd,CM)	0.83	0.80	0.85	0.83	0.73	0.71	0.66	0.46

Scheme 5

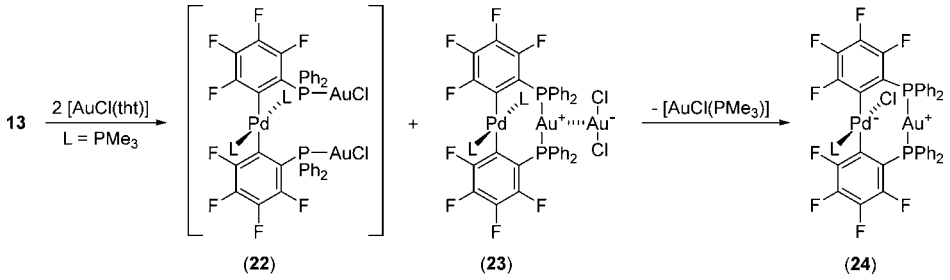

and CM atoms are in general positive and, in the case of Pd, relatively constant. The NCs of the coinage metal atoms strongly depend on the metal and on the CM-bound counterion. Interestingly, upon formation of cationic complexes (i.e., transition from chloro compounds **14**−**16** to the corresponding hexafluorophosphates **17**−**19**, respectively) the positive NC of the CM decreases. As the NCs of the ligand donor atoms P_{CM} are relatively unaffected by this change, the excess cationic charge of the complex must be delocalized toward the periphery of the molecule. As shown in Table 4, the Pd···CM separations are systematically shorter for the complexes with a less positive sum of the calculated NCs of the metal atoms. This observation is in agreement with a model in which intermetallic Coulombic repulsions are outweighed by attractive noncovalent intermetallic (dispersion) interactions.

In principle, adduct formation of **13** with 2 equiv of coinage metal halide should be possible, especially with soluble metal halide sources {such as [AuCl(tht)]}. When a CH_2Cl_2 solution of **13** was treated with 2 equiv of [AuCl(tht)] and the ^{31}P NMR spectrum recorded immediately, a pair of equally intense multiplet resonances at δ 36.2 and −17.6 was observed, presumably due to the trinuclear species $[(Me_3P)_2Pd(\mu\text{-}2\text{-}C_6F_4PPh_2)_2(AuCl)_2]$ (**22**) (Scheme 5). Also present was a second pair of low intensity resonances at δ 33.4 and −21.6 due to the rearranged product $[(Me_3P)_2Pd(\mu\text{-}2\text{-}C_6F_4PPh_2)_2Au][AuCl_2]$ (**23**), the X-ray structure of which is shown in Figure 9; attempts to obtain crystals of **22** were unsuccessful. The products were unstable in solution and over time the intensities of the peaks due to **22** decreased and those of **23** increased; in addition, new multiplet resonances at δ 35.8 and −5.4 and a sharp singlet at δ −9.9 in a 2:1:1 ratio appeared. After 24 h, the resonances due to **22** and **23** had completely disappeared, and only those of the new species remained. The resonances at δ 35.8 and −5.4 are assigned to the binuclear zwitterionic complex $[(Me_3P)PdCl(\mu\text{-}2\text{-}C_6F_4PPh_2)_2Au]$ (**24**), the structure

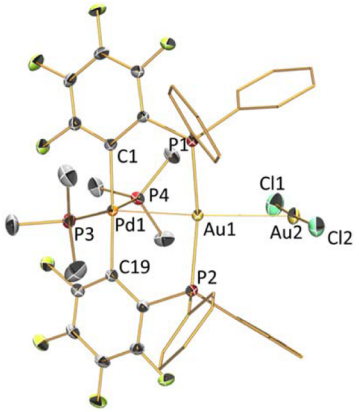

Figure 9. Molecular structure of $[(Me_3P)_2Pd(\mu\text{-}2\text{-}C_6F_4PPh_2)_2Au][AuCl_2]$ (**23**). Ellipsoids show 50% probability levels. Hydrogen atoms have been omitted and phenyl groups are depicted as stick models for clarity. Selected bond lengths (Å) and angles (deg): Pd(1)···Au(1) 2.8301(2), Au(1)···Au(2) 2.94767(15), Pd(1)−C(1) 2.0692(18), Pd(1)−C(19) 2.0746(18), Pd(1)−P(3) 2.3118(5), Pd(1)−P(4) 2.3196(5), Au(1)−P(1) 2.3217(5), Au(1)−P(2) 2.3231(5), P(1)−Au(1)−P(2) 166.826(18), C(1)−Pd(1)−C(19) 176.84(7), P(3)−Pd(1)−P(4) 166.18(2), C(1)−Pd(1)−P(3) 90.54(5), C(1)−Pd(1)−P(4) 87.96(5), C(19)−Pd(1)−P(3) 89.99(5), C(19)−Pd(1)−P(4) 90.79(5).

of which was confirmed by X-ray crystallography and is shown in Figure 10. Complex **24** is formed from **23** by elimination of [AuCl(PMe$_3$)], which is responsible for the sharp singlet at δ −9.9 (δ_{CDCl_3} −9.7).[40]

The heterobimetallic complex $[(Me_3P)PdCl(\mu\text{-}2\text{-}C_6F_4PPh_2)_2Au]$ (**24**) could also be obtained directly from the reaction of *trans*-$[Pd(\kappa^2\text{-}2\text{-}C_6F_4PPh_2)_2]$ (**7**) with [AuCl(PMe$_3$)]. Complex **7** also undergoes reaction with [AuCl(PPh$_3$)] to give a binuclear product of composition $[(Ph_3P)$-

DOI: 10.1021/acs.inorgchem.5b00939
Inorg. Chem. 2015, 54, 6947−6957

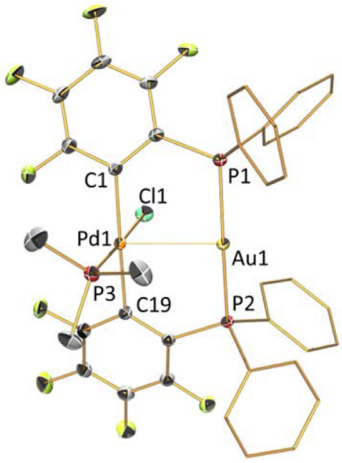

Figure 10. Molecular structure of $[(Me_3P)PdCl(\mu\text{-}2\text{-}C_6F_4PPh_2)_2Au]$ (**24**). Ellipsoids show 50% probability levels. For clarity, hydrogen atoms have been omitted and phenyl groups are depicted as stick models. Selected bond lengths (Å) and angles (deg): Pd(1)···Au(1) 2.8013(3), Pd(1)−C(1) 2.077(3), Pd(1)−C(19) 2.065(3), Pd(1)−P(3) 2.2187(8), Pd(1)−Cl(1) 2.3856(8), Au(1)−P(1) 2.3025(8), Au(1)−P(2) 2.3066(7), P(1)−Au(1)−P(2) 174.46(3), C(1)−Pd(1)−C(19) 174.35(11), P(3)−Pd(1)−Cl(1) 178.04(3), C(1)−Pd(1)−P(3) 92.18(8), C(1)−Pd(1)−Cl(1) 89.11(8), C(19)−Pd(1)−P(3) 93.12(8), C(19)−Pd(1)−Cl(1) 85.54(8).

$PdCl(\mu\text{-}2\text{-}C_6F_4PPh_2)_2Au]$ (**25**) (Scheme 6), the X-ray structure of which is shown in Figure 11. The two bridging $C_6F_4PPh_2$ groups are mutually *cis* in a head-to-tail arrangement about the palladium atom, whereas in **24** they are mutually *trans* in a head-to-head arrangement about palladium. The ^{31}P NMR spectrum of **25** shows a pair of multiplet resonances at δ 47.8 and 23.8 in a 1:2 ratio; the downfield resonance can be assigned to the phosphorus atom in $C_6F_4PPh_2$ bound to gold and the upfield resonance to overlapping peaks due to the $C_6F_4PPh_2$ and PPh_3 ligands bound to palladium. Curiously, in the solution ^{31}P NMR spectrum, the large coupling (ca. 400 Hz) that would be expected between the mutually *trans*-phosphorus atoms in the PPh_3 and μ-$C_6F_4PPh_2$ groups was not observed, which is apparently inconsistent with the observed solid state structure. There appear to be three possible explanations for this behavior. First, in solution, the head-to-tail arrangement of **25** (Scheme 6) is retained, but the positions of PPh_3 and Cl are interchanged. Alternatively, the solution structure may be analogous to that of **24**, containing head-to-head $C_6F_4PPh_2$ groups, but this spontaneously isomerizes on crystallization to the structure shown in Scheme 6. As there was no evidence for the coexistence of isomers in solution, and computational analyses predict the crystallographically observed isomer of **25**

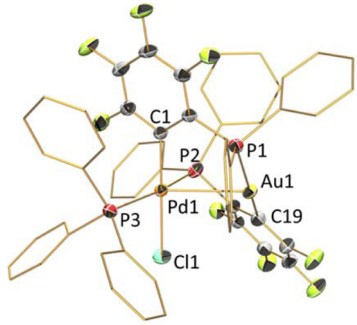

Figure 11. Molecular structure of $[(Ph_3P)PdCl(\mu\text{-}2\text{-}C_6F_4PPh_2)_2Au]$ (**25**). Ellipsoids show 50% probability levels. Hydrogen atoms have been omitted and phenyl groups are depicted as stick models for clarity. Selected bond lengths (Å) and angles (deg): Pd(1)···Au(1) 2.93828(18), Pd(1)−C(1) 2.0226(17), Pd(1)−P(2) 2.3660(5), Pd(1)−P(3) 2.3429(5), Pd(1)−Cl(1) 2.3773(5), Au(1)−P(1) 2.2783(5), Au(1)−C(19) 2.0534(18), C(19)−Au(1)−P(1) 167.05(5), C(1)−Pd(1)−Cl(1) 178.05(5), P(2)−Pd(1)−P(3) 165.479(17), C(1)−Pd(1)−P(2) 93.59(5), C(1)−Pd(1)−P(3) 89.57(5), Cl(1)−Pd(1)−P(2) 88.02(2), Cl(1)−Pd(1)−P(3) 89.044(19).

to be more stable than alternative isomers with head-to-head bridges or *cis*-phosphines at palladium (vide infra), we favor the third explanation, namely, that the very similar chemical shifts of the mutually *trans* pair of ^{31}P nuclei ($\Delta\delta$ very small), render the signal splitting due to P−P coupling unobservable.

The basic geometry and metrical parameters in $[(Me_3P)_2Pd(\mu\text{-}2\text{-}C_6F_4PPh_2)_2Au][AuCl_2]$ (**23**), $[(Me_3P)PdCl(\mu\text{-}2\text{-}C_6F_4PPh_2)_2Au]$ (**24**), and $[(Me_3P)_2Pd(\mu\text{-}2\text{-}C_6F_4PPh_2)_2Au]PF_6$ (**19**) are generally similar to those observed in **14**−**16**, the main differences being the Pd···Au separations and associated angles about the metal centers. In the molecular structure of **23** (Figure 9), the distance between the two metal atoms is only 2.8301(2) Å, which is significantly less than that observed in **16**; in **24** (Figure 10) this separation is even smaller, 2.8013(3) Å, and already very similar to the Pd···Au separation in the cationic complex **19**, 2.7970(4) Å. This is remarkable, because in **24** the gold atom Au1 still exhibits strong interaction with the counterion, i.e., an aurophilic contact Au1···Au2 with a separation of 2.9477(2) Å, which is only slightly longer than the interatomic separation observed in metallic gold (2.884 Å).[41]

As expected, the geometry about the palladium atom in complex **25** is approximately square planar, while that at gold is approximately linear, albeit more distorted from linearity than that observed in **24** [167.05(5)° vs 174.46(3)°]. This distortion, together with a slight twist in one of the bridging metalated phosphine ligands, results in a Pd···Au separation of 2.9383(2) Å, significantly greater than that in **24** [2.8013(3) Å].

Scheme 6

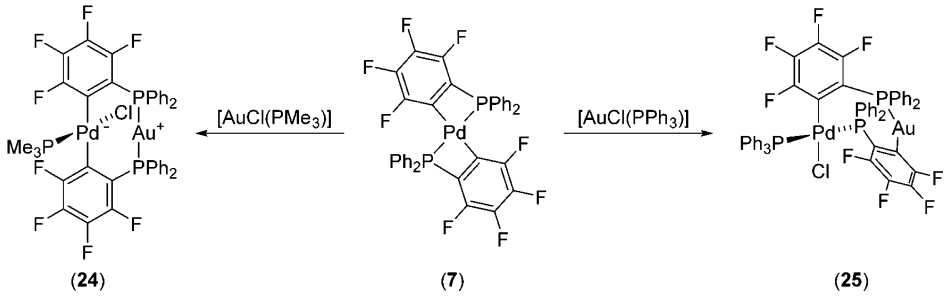

DOI: 10.1021/acs.inorgchem.5b00939
Inorg. Chem. 2015, 54, 6947−6957

Scheme 7

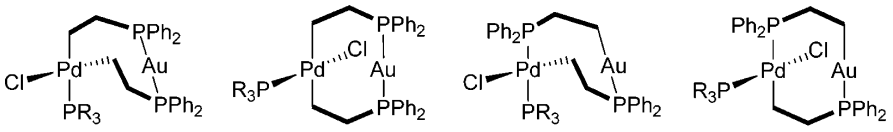

As one could expect the different coordination modes found in compounds **24** and **25** (head-to-head bridging, *hh* vs head-to-tail bridging, *ht*; *cis*- vs *trans*-arrangement of the bridging ligands in the Pd coordination sphere) to originate from different thermodynamic stabilities of the isomers, depending on the monodentate phosphine bound to Pd (PMe_3 vs PPh_3), we calculated the binding energies of the four isomers depicted in Scheme 7 for the compounds with PR_3 = PMe_3 and PPh_3 (Table 5). Interestingly, in both cases the *ht-cis* isomer is noticeably more stable than the other three isomers. For compound **25** this is in accord with the experimentally found molecular configuration, and it underlines that the *ht-cis* isomer of **25** should be the favored isomer is solution (*vide supra*). For compound **24**, however, the experimentally found *hh-trans* isomer is predicted to be about 6 kcal mol^{-1} less stable than its *ht-cis* isomer. Thus, we suggest that *hh-trans*-**24** is kinetically stabilized owing to the reluctance of PMe_3 to dissociate from the coordination sphere.

Table 5. Calculated relative energies of the isomers *hh-cis*, *hh-trans*, *ht-cis*, and *ht-trans* of compounds 24 (PR_3 = PMe_3) and 25 (PR_3 = PPh_3) in kcal/mol

	24	25
hh-cis	17.0	15.7
hh-trans	6.3	10.1
ht-cis	0.0	0.0
ht-trans	5.0	6.8

CONCLUSIONS

The complex *trans*-[Pd(κC-2-$C_6F_4PPh_2$)$_2$(PMe_3)$_2$] (**13**), prepared from *trans*-[Pd(κ^2-2-$C_6F_4PPh_2$)$_2$] and PMe_3, has been shown to act as a *trans*-spanning bidentate ligand by coordination of the PPh_2 groups to a second metal atom. Thus, treatment of **13** with MCl (M = Cu, Ag, Au) gave the complexes [(Me_3P)$_2$Pd(μ-2-$C_6F_4PPh_2$)$_2$MCl] [M = Cu (**14**), Ag (**15**), Au (**16**)] with metal−metal separations in the range of 2.8448(3)−2.9170(4) Å. Generation of the cationic complexes [(Me_3P)$_2$Pd(μ-2-$C_6F_4PPh_2$)$_2$M]PF_6 [M = Cu (**17**), Ag (**18**), Au (**19**)] by abstraction of the chloro ligands by $TlPF_6$ resulted in a 0.05−0.08 Å contraction of the metal−metal separation. These short metal−metal separations [2.7707(11)−2.86819(18) Å] are consistent with the presence of a metallophilic interaction between the d^8 and d^{10} metal atoms. Natural bond orbital (NBO) and natural localized molecular orbital (NLMO) calculations on complexes **14**−**21** indicate the absence of shared electron pairs between the metal atoms. Furthermore, electron localization function (ELF) calculations on complexes **16** and **19** did not reveal any electron density localization between the two metal atoms. The presence of attractive, noncovalent (dispersion) interactions between the metal atoms, consistent with the observations of short Pd···M separations in the solid state crystal structures, was revealed by analysis of the noncovalent interactions descriptor (NCI); this interaction was more pronounced in **19** compared to **16**, consistent with the shorter Pd···Au separation [**16**: 2.8842(4) Å; **19**: 2.7970(4) Å]. For all complexes studied, a shortening of the Pd···M (M = Cu, Ag, Au) separation, accompanied by a lowering of the positive natural charge (NC) of the Pd-M core, was observed thus highlighting the interplay of the attractive dispersion forces and the repulsive electrostatic forces in these heterobinuclear complexes.

EXPERIMENTAL SECTION

General Comments. Hexane and dichloromethane were dried by passage through standard solvent drying columns. The compounds *trans*-[Pd(κ^2-2-$C_6F_4PPh_2$)$_2$],[21] [AuCl(tht)],[42] and [AuCl(PPh_3)][43] were prepared by literature methods, and all other reagents were commercially available and used as received. ^{1}H (300 MHz), ^{19}F (282 MHz), and ^{31}P (121 MHz) NMR spectra were measured on a Bruker Avance 300 spectrometer at room temperature in CD_2Cl_2, unless otherwise stated. Coupling constants (J) are given in Hertz (Hz) and chemical shifts (δ) in ppm, internally referenced to residual solvent signals (^{1}H), $CFCl_3$ (^{19}F) or external 85% H_3PO_4 (^{31}P). The separations reported below as coupling constants J_{PH} for the PMe_3 triplets are in fact ($^2J_{PH}$ + $^4J_{PH}$). Elemental analyses were carried out by the Microanalytical Unit at the Research School of Chemistry, ANU.

X-ray Crystallography. Crystals suitable for X-ray crystallography were obtained from dichloromethane (*anti*-**13**), d_2-dichloromethane (**20**), methanol (**16**), benzene (**18**), dichloromethane/methanol (*syn*-**13**, **14**, **15**, **23**−**25**), dichloromethane/hexane (**21**), or THF/ether (**19**). The crystals were selected under nujol and mounted on a glass capillary with a thin film of silicon grease. Data were collected on a D8 Bruker diffractometer equipped with an Apex II CCD detector using graphite monochromated Mo Kα radiation (λ = 0.71073 Å) from a 1 μS microsource. Geometric and intensity data were collected using SMART software.[44] The data were processed using SAINT,[45] and corrections for absorption were applied using SADABS.[46] The structures were solved by direct methods and refined with full-matrix least-squares methods of F^2 using the SHELXTL package.[47] Parameters of data collection and structure refinement of the crystal structures discussed in this paper are reported in the Supporting Information. CIF files have been deposited with the Cambridge Crystallographic Data Center (CCDC) and can be obtained free of charge (for inquiry contact: CCDC, 12 Union Road, Cambridge, CB2 1EZ, UK, fax: +44−1223−336033, e-mail: deposit@ccdc.cam.ac.uk) quoting the following reference numbers: CCDC-955874 (*syn*-**13**), CCDC-955876 (*anti*-**13**), CCDC-1051745 (**14**), CCDC-1051746 (**15**), CCDC-955877 (**16**), CCDC-1051747 (**17**·2.25 THF), CCDC-1051748 (**18**·2.5 C_6H_6), CCDC-955880 (**19**), CCDC-1051749 (**20**·CH_2Cl_2), CCDC-1051750 (**21**), CCDC-955878 (**23**·CH_2Cl_2), CCDC-955875 (**24**·0.5 C_6H_6) and CCDC-955879 (**25**).

Computational Analyses. Calculations were carried out using density functional theory (DFT) methodology as implemented in adf2013.01c;[48−50] Perdew−Burke−Ernzerhof (PBE)[51] functional with D3 correction[52] for the weak van der Waals interaction was used to optimize the geometries. The basis set used was all electron TZ2P[53] optimized to be used in zeroth-order regular approximation (ZORA),[54−57] which accounts also for relativistic effects (scalar relativistic). For NBO/NLMO analyses of compounds **14**−**21** the

DOI: 10.1021/acs.inorgchem.5b00939
Inorg. Chem. 2015, 54, 6947−6957

atomic coordinates of the non-hydrogen atoms have been retained, but the positions of the hydrogen atoms have been optimized. For further analyses of the electronic features of the Au−Pd compounds **16** and **19** (ELF, NCI) and for the energetic comparison of the *hh-cis*, *hh-trans*, *ht-cis*, and *ht-trans* isomers of **24** and **25** their molecular structures have been completely optimized in the gas phase. (The fully optimized geometries reasonably reproduce the X-ray structures but possess slightly twisted geometries, possibly due to the missing crystal environment.) The integrals were evaluated with an accuracy of five significant digits and use of an energy convergence criterion of 1 e^{-5}.

The NBO/NLMO calculations were carried out using the NBO6 program[58] using the electronic densities from the partially (H atoms) optimized compounds.

The ELF[59] and non-covalent index (NCI)[60] were used to investigate the electron density features along the Au−Pd axes and in their vicinity in the fully optimized molecular structures. For ELF and NCI, the PBE functional was replaced by B3LYP[61,62] functional to compute better quality electron density distributions.

Syntheses. *syn- and anti-[Pd(κC-2-$C_6F_4PPh_2$)$_2$(PMe_3)$_2$] (**13**).* To a solution of *trans*-[Pd(κ^2-2-$C_6F_4PPh_2$)$_2$] (145 mg, 0.19 mmol) in CH_2Cl_2 (15 mL) was added PMe_3 (1.0 M solution in toluene, 560 μL, 0.56 mmol). After the mixture was stirred at ambient temperature for 1 h, the solvent was removed *in vacuo*. The white residue was stirred in methanol (10 mL), filtered, washed with methanol (5 mL), and air-dried (156 mg, 90%). ^{1}H NMR (C_6D_6): δ 0.47 (br. s, 18H, Me), 6.95−7.12 (m, 12H, aromatic), 7.53−7.64 (m, 1H, aromatic), 7.64−7.80 (m, 7H, aromatic). ^{19}F NMR (C_6D_6): δ −111.1 (m), −118.1 (m), −154.0 (m), −159.6 (m) (minor isomer); −111.4 (m), −120.3 (m), −154.4 (m), −159.5 (m) (major isomer). ^{31}P NMR (C_6D_6): δ −2.9 (m), −19.1 (m) (minor isomer); −8.4 (m), −18.7 (m) (major isomer). Estimated *syn:anti* ratio ca. 1:6. Anal. Calcd for $C_{42}H_{38}F_8P_4Pd$: C 54.53, H 4.14, F 16.43. Found: C 54.91, H 4.26, F 16.21.

*[(Me_3P)$_2$Pd(μ-2-$C_6F_4PPh_2$)$_2$CuCl] (**14**).* To a solution of **13** (100 mg, 0.11 mmol) in CH_2Cl_2 (20 mL) was added solid CuCl (10.7 mg, 0.11 mmol). The mixture was stirred overnight and filtered through Celite. Methanol was added to the solution and the volume was reduced *in vacuo*. The precipitated white solid was isolated by filtration, washed with methanol, and dried *in vacuo* (85 mg, 77%). ^{1}H NMR: δ 0.98 (t, J_{PH} 3.7 Hz, 18H, Me), 7.25−7.54 (m, 20H, aromatic). ^{19}F NMR: δ −109.8 (m), −118.6 (m), −151.8 (m), −159.7 (m). ^{31}P NMR: δ 3.1 (br. m), −16.6 (m). Anal. Calcd for $C_{42}H_{38}ClCuF_8P_4Pd$: C 49.26, H 3.74, Cl 3.46, F 14.84. Found: C 49.44, H 3.71, Cl 3.41, F 14.99.

*[(Me_3P)$_2$Pd(μ-2-$C_6F_4PPh_2$)$_2$AgCl] (**15**).* To a solution of **13** (50 mg, 0.05 mmol) in CH_2Cl_2 (20 mL) was added solid AgCl (7.8 mg, 0.05 mmol), and the mixture was stirred in the dark. After 2 h, more AgCl (2 mg, 0.01 mmol) was added and stirring was continued overnight. The turbid solution was filtered through Celite, methanol was added to the filtrate, and the volume was reduced *in vacuo*. The white precipitate was filtered off, washed with methanol, and dried *in vacuo* (48 mg, 83%). ^{1}H NMR: δ 0.92 (t, J_{PH} 3.6 Hz, 18H, Me), 7.33−7.48 (m, 12H, aromatic), 7.53−7.63 (m, 8H, aromatic). ^{19}F NMR: δ −107.9 (m), −119.4 (m), −151.5 (m), −159.1 (m). ^{31}P NMR: δ 11.8 (dm, J_{AgP} 438 Hz), −17.7 (m). Anal. Calcd for $C_{42}H_{38}AgClF_8P_4Pd$: C 47.22, H 3.58, F 14.23. Found: C 47.47, H 3.61, F 14.17.

*[(Me_3P)$_2$Pd(μ-2-$C_6F_4PPh_2$)$_2$AuCl] (**16**).* To a solution of **13** (100 mg, 0.11 mmol) in CH_2Cl_2 (20 mL) was added solid [AuCl(tht)] (35 mg, 0.11 mmol), and the mixture was stirred for 2 h. The solvent was removed *in vacuo*, and the residue was dissolved in methanol. After the suspension had been filtered through Celite, the solvent was evaporated and the white solid was washed with hexane and dried *in vacuo* (81 mg, 65%). ^{1}H NMR: δ 0.93 (t, J_{PH} 3.6 Hz, 18H, Me), 7.38−7.58 (m, 12H, aromatic), 7.63−7.77 (m, 8H, aromatic). ^{19}F NMR: δ −105.6 (m), −118.1 (m), −149.3 (m), −158.5 (m). ^{31}P NMR: δ 37.9 (br. m), −17.7 (br. m). Anal. Calcd for $C_{42}H_{38}AuClF_8P_4Pd$: C 43.58, H 3.31, Cl 3.06, F 13.13. Found: C 43.69, H 3.37, Cl 3.19, F 13.34.

*[(Me_3P)$_2$Pd(μ-2-$C_6F_4PPh_2$)$_2$Cu]PF_6 (**17**).* To a solution of **13** (63 mg, 0.06 mmol) in CH_2Cl_2 (20 mL) was added solid $TlPF_6$ (24 mg, 0.07 mmol), and the mixture was stirred overnight. After filtration of the mixture through Celite, the solvent was removed *in vacuo* and the residue was suspended in hexane. The white product was isolated by filtration, washed with hexane, and dried *in vacuo* (61 mg, 87%). ^{1}H NMR: δ 0.98 (t, J_{PH} 3.5 Hz, 18H, Me), 7.41−7.66 (m, 20H, aromatic). ^{19}F NMR: δ −73.2 (d, J_{PF} 710 Hz, PF_6), −110.4 (m), −118.7 (m), −147.5 (m), −156.9 (m). ^{31}P NMR: δ 11.7 (m), −14.5 (m), −144.5 (sept, J_{PF} 711 Hz, PF_6). Anal. Calcd for $C_{42}H_{38}CuF_{14}P_5Pd$: C 44.50, H 3.38, F 23.46. Found: C 44.74, H 3.38, F 22.99.

*[(Me_3P)$_2$Pd(μ-2-$C_6F_4PPh_2$)$_2$Ag]PF_6 (**18**).* (a) This was made analogously to **17** from **13** (10 mg, 0.01 mmol) and $TlPF_6$ (4 mg, 0.01 mmol) to give the product as a white solid (10 mg, 90%). ^{1}H NMR: δ 0.94 (t, J_{PH} 3.4 Hz, 18H, Me), 7.47−7.65 (m, 20H, aromatic). ^{19}F NMR: δ −73.1 (d, J_{PF} 711 Hz, PF_6), −107.6 (m), −117.3 (m), −148.0 (m), −156.9 (m). ^{31}P NMR: δ 18.6 (dm, J_{AgP} 531 Hz), −16.1 (m), −144.5 (sept, J_{PF} 711 Hz, PF_6). Anal. Calcd for $C_{42}H_{38}AgF_{14}P_5Pd$: C 42.83, H 3.25, F 22.58. Found: C 43.10, H 3.09, F 22.42.

(b) Complex **18** could also be prepared in a less pure state by stirring a mixture of **13** (50 mg, 0.05 mmol) and $AgPF_6$ (14 mg, 0.05 mmol) in CH_2Cl_2 (20 mL) overnight, shielded from light. Addition of hexane to the solution and partial evaporation gave **18** as a slightly brown solid (48 mg, 75%).

*[(Me_3P)$_2$Pd(μ-2-$C_6F_4PPh_2$)$_2$Au]PF_6 (**19**).* This was made similarly to **17** from **16** (30 mg, 0.03 mmol) dissolved in methanol (20 mL) and $TlPF_6$ (10 mg, 0.03 mmol) to give the product as a white solid (29 mg, 88%). ^{1}H NMR: δ 0.96 (t, J_{PH} 3.5 Hz, 18H, Me), 7.50−7.68 (m, 20H, aromatic). ^{19}F NMR: δ −73.2 (d, J_{PF} 711 Hz, PF_6), −105.9 (m), −117.7 (m), −147.1 (m), −157.2 (m). ^{31}P NMR: δ 40.8 (m), −16.6 (m), −144.5 (sept, J_{PF} 711 Hz, PF_6). Anal. Calcd for $C_{42}H_{38}AuF_{14}P_5Pd$: C 39.82, H 3.02, F 20.99. Found: C 39.79, H 3.01, F 21.09.

*[(Me_3P)$_2$Pd(μ-2-$C_6F_4PPh_2$)$_2$Ag]OTf (**20**).* To a solution of **13** (15 mg, 0.02 mmol) in CD_2Cl_2 (0.7 mL) was added solid AgOTf (4.2 mg, 0.02 mmol). Addition of hexane and slow evaporation in the dark afforded white crystals, which were separated by decantation, washed with hexane, and air-dried (16 mg, 78%). ^{1}H NMR: δ 0.91 (t, J_{PH} 3.4 Hz, 18H, Me), 7.38−7.70 (m, 20H, aromatic). ^{19}F NMR: δ −78.8 (s, OTf), −107.7 (m), −118.0 (m), −149.4 (m), −157.7 (m). ^{31}P NMR: δ 16.6 (dm, J_{AgP} 521 Hz), −16.8 (m). Anal. Calcd for $C_{43}H_{38}AgF_{11}O_3P_4PdS{\cdot}0.85CD_2Cl_2$: C 41.99, H 3.33, Cl 4.74, F 16.68, S 2.55. Found: C 42.06, H 3.47, Cl 4.53, F 16.27, S 2.44.

*[(Me_3P)$_2$Pd(μ-2-$C_6F_4PPh_2$)$_2$Ag]$OOCCF_3$ (**21**).* This was made analogously to **20** above from **13** (15 mg, 0.02 mmol) and $AgOOCCF_3$ (3.6 mg, 0.02 mmol) in CD_2Cl_2 (0.07 mL) to give the title product (17.5 mg, 88%). ^{1}H NMR: δ 0.88 (t, J_{PH} 3.4 Hz, 18H, Me), 7.31−7.47 (m, 12H, aromatic), 7.50−7.63 (m, 8H, aromatic). ^{19}F NMR: δ −74.7 (s, CF_3COO), −107.8 (m), −119.2 (m), −151.0 (m), −158.7 (m). ^{31}P NMR: δ 14.8 (dm, J_{AgP} 497 Hz), −17.6 (m). Anal. Calcd for $C_{43}H_{38}AgF_{11}O_3P_4PdS{\cdot}0.7CD_2Cl_2$: C 44.49, H 3.41, Cl 4.11, F 17.32. Found: C 44.41, H 3.06, Cl 4.12, F 17.67.

*[(Me_3P)$_2$Pd(μ-2-$C_6F_4PPh_2$)$_2$($AuCl)_2$] (**22**) and [(Me_3P)$_2$Pd(μ-2-$C_6F_4PPh_2$)$_2$Au][$AuCl_2$] (**23**).* To an NMR tube containing **13** (13 mg, 0.014 mmol), CH_2Cl_2 (0.8 mL) and a glass capillary containing C_6D_6 was added [AuCl(tht)] (9 mg, 0.028 mmol), and the reaction was monitored by ^{19}F and ^{31}P NMR spectroscopy. Selected data for **22**: ^{19}F NMR (CH_2Cl_2/C_6D_6): δ −106.0 (m), −117.4 (m), −148.6 (m), −158.0 (m). ^{31}P NMR (CH_2Cl_2/C_6D_6): δ 36.2 (m), −17.6 (m). Selected data for **23**: ^{19}F NMR (CH_2Cl_2/C_6D_6): δ −88.1 (m), −116.5 (m), −148.8 (m), −159.1 (m). ^{31}P NMR (CH_2Cl_2/C_6D_6): δ 33.4 (m), −21.6 (m). Selected data for **24**: ^{19}F NMR (CH_2Cl_2/C_6D_6): δ −110.4 (m), −121.6 (m), −150.5 (m), −161.4 (m). ^{31}P NMR (CH_2Cl_2/C_6D_6): δ 35.7 (m), −5.4 (m).

*[(Me_3P)PdCl(μ-2-$C_6F_4PPh_2$)$_2$Au] (**24**).* (a) A solution of **13** (70 mg, 0.075 mmol) and [AuCl(tht)] (48 mg, 0.15 mmol) in CH_2Cl_2 (20 mL) was stirred overnight. The solvent was removed *in vacuo*, and the white residue was washed with methanol and dried *in vacuo* (59 mg, 72%). ^{1}H NMR (C_6D_6): δ 0.47 (d, J_{PH} 10.7 Hz, 9H, Me), 6.83−7.20 (m, 12H, aromatic), 7.51−7.72 (m, 4H, aromatic), 8.01−8.23 (m, 4H, aromatic). ^{19}F NMR (C_6D_6): δ −109.0 (m), −122.2 (m), −149.5 (m), −160.4 (m). ^{31}P NMR (C_6D_6): δ 35.7 (m, 2P), −7.6 (m, 1P). Anal.

DOI: 10.1021/acs.inorgchem.5b00939
Inorg. Chem. 2015, 54, 6947−6957

Calcd for $C_{39}H_{29}AuClF_8P_3Pd$: C 43.32, H 2.70, Cl 3.28, F 14.05. Found: C 43.30, H 2.67, Cl 3.12, F 13.79.

(b) A solution containing *trans*-[Pd(κ^2-2-$C_6F_4PPh_2$)$_2$] (50 mg, 0.07 mmol) and [AuCl(PMe_3)] (20 mg, 0.07 mmol) in CH_2Cl_2 (20 mL) was stirred overnight. Addition of methanol and evaporation at reduced pressure precipitated the product as a white solid, which was filtered off, washed with methanol, and dried *in vacuo* (48 mg, 68%). The spectroscopic data were identical to those reported for (a) above.

*[(Ph_3P)PdCl(μ-2-$C_6F_4PPh_2$)$_2$Au] (**25**).* To a solution of *trans*-[Pd(κ^2-2-$C_6F_4PPh_2$)$_2$] (30 mg, 0.04 mmol) in CH_2Cl_2 (20 mL) was added solid [AuCl(PPh_3)] (19 mg, 0.04 mmol), and the mixture was stirred overnight. Addition of hexane and slow evaporation gave yellow crystals, which were isolated by decantation, washed with hexane, and dried *in vacuo* (81 mg, 95%). ^{1}H NMR (C_6D_6): δ 6.12−6.29 (m, 4H, aromatic), 6.52−7.06 (m, 23H, aromatic), 7.83−7.98 (m, 4H, aromatic), 8.41−8.59 (m, 4H, aromatic). ^{19}F NMR (C_6D_6): δ −101.4 (m), −113.5 (m), −118.8 (m), −128.6 (m), −149.6 (m), −150.9 (m), −157.9 (m), −160.9 (m). ^{31}P NMR (C_6D_6): δ 47.8 (m, 1P), 23.8 (m, 2P). Anal. Calcd for $C_{54}H_{35}AuClF_8P_3Pd$: C 51.17, H 2.78, Cl 2.80, F 11.99. Found: C 51.33, H 2.61, Cl 2.87, F 12.35.

■ ASSOCIATED CONTENT

Supporting Information

Crystallographic information file. Parameters of data collection and structure refinement for the structures of *syn*-**13**, *anti*-**13**, **14**, **15**, **16**, **17**·2.25 THF, **18**·2.5 C_6H_6, **19**, **20**·CH_2Cl_2, **21**, **23**·CH_2Cl_2, **24**·0.5 C_6H_6, and **25**. Atomic coordinates and molecular representations of the calculated isomers (*hh-cis*, *hh-trans*, *ht-cis*, and *ht-trans*) of complexes **24** and **25**. The Supporting Information is available free of charge on the ACS Publications website at DOI: 10.1021/acs.inorgchem.5b00939.

■ AUTHOR INFORMATION

Corresponding Author

*E-mail: suresh.bhargava@rmit.edu.au.

Notes

The authors declare no competing financial interest.

■ ACKNOWLEDGMENTS

The authors thank M.Sc. Robert Gericke for crystallographic analysis of compound **15**.

■ REFERENCES

(1) Xia, B.-H.; Zhang, H.-X.; Che, C.-M.; Leung, K.-H.; Phillips, D. L.; Zhu, N.; Shou, Z.-Y. *J. Am. Chem. Soc.* **2003**, *125*, 10362 and references cited therein.

(2) Liu, T.; Zhou, X.; Zhang, H.-X.; Xia, B.-H. *Dalton Trans.* **2008**, 1065 and references cited therein.

(3) Lasanta, T.; López-de-Luzuriaga, J. M.; Monge, M.; Olmos, M. E.; Pascual, D. *Chem.—Eur. J.* **2013**, *19*, 4754.

(4) López-de-Luzuriaga, J. M.; Monge, M.; Olmos, M. E.; Pascual, D. *Inorg. Chem.* **2014**, *53*, 1275.

(5) Hupf, E.; Lork, E.; Mebs, S.; Beckmann, J. *Inorg. Chem.* **2015**, *54*, 1847.

(6) Doerrer, L. H. *Dalton Trans.* **2010**, *39*, 3543.

(7) Sculfort, S.; Braunstein, P. *Chem. Soc. Rev.* **2011**, *40*, 2741.

(8) Laguna, A., Ed. *Modern Supramolecular Gold Chemistry*; Wiley-VCH: Weinheim, Germany, 2008; Chapters 2 and 4.

(9) Puddephatt, R. J. *Chem. Soc. Rev.* **1983**, *12*, 99.

(10) Chaudret, B.; Delavaux, B.; Poilblanc, R. *Coord. Chem. Rev.* **1988**, *86*, 191.

(11) Hutton, A. T.; Pringle, P. G.; Shaw, B. L. *Organometallics* **1983**, *2*, 1889.

(12) Balch, A. L.; Catalano, V. J.; Olmstead, M. M. *Inorg. Chem.* **1990**, *29*, 585.

(13) Cooper, G. R.; Hulton, A. T.; Langrick, C. R.; McEwan, D. M.; Pringle, P. G.; Shaw, B. L. *J. Chem. Soc., Dalton Trans.* **1984**, 855.

(14) Hassan, F. S. M.; Markham, D. P.; Pringle, P. G.; Shaw, B. L. *J. Chem. Soc., Dalton Trans.* **1985**, 279.

(15) Yip, H.-K.; Lin, H.-M.; Cheung, K.-K.; Che, C.-M.; Wang, Y. *Inorg. Chem.* **1994**, *33*, 1644.

(16) Fernández, E. J.; López-de-Luzuriaga, J. M.; Monge, M.; Rodríguez, M. A.; Crespo, O.; Gimeno, C.; Laguna, A.; Jones, P. G. *Chem.—Eur. J.* **2000**, *6*, 636.

(17) Crespo, O.; Laguna, A.; Fernández, E. J.; López-de-Luzuriaga, J. M.; Jones, P. G.; Teichert, M.; Monge, M.; Pyykkö, P.; Runeberg, N.; Schütz, M.; Werner, H.-J. *Inorg. Chem.* **2000**, *39*, 4786.

(18) Yip, H.-K.; Che, C.-M.; Ping, S.-M. *J. Chem. Soc., Chem. Commun.* **1991**, 1626.

(19) Balch, A. L.; Catalano, V. J. *Inorg. Chem.* **1991**, *30*, 1302.

(20) Bennett, M. A.; Bhargava, S. K.; Ke, M.; Willis, A. C. *J. Chem. Soc., Dalton Trans.* **2000**, 3537.

(21) Bennett, M. A.; Bhargava, S. K.; Keniry, M. A.; Privér, S. H.; Simmonds, P. M.; Wagler, J.; Willis, A. C. *Organometallics* **2008**, *27*, 5361.

(22) Bennett, M. A.; Bhargava, S. K.; Messelhäuser, J.; Privér, S. H.; Welling, L. L.; Willis, A. C. *Dalton Trans.* **2007**, 3158.

(23) Bhargava, S. K.; Privér, S. H.; Willis, A. C.; Bennett, M. A. *Organometallics* **2012**, *31*, 5561.

(24) Bennett, M. A.; Bhargava, S. K.; Griffiths, K. D.; Robertson, G. B.; Wickramasinghe, W. A.; Willis, A. C. *Angew. Chem., Int. Ed. Engl.* **1987**, *26*, 258.

(25) Bennett, M. A.; Bhargava, S. K.; Hockless, D. C. R.; Welling, L. L.; Willis, A. C. *J. Am. Chem. Soc.* **1996**, *118*, 10469.

(26) Bennett, M. A.; Bhargava, S. K.; Mirzadeh, N.; Privér, S. H.; Wagler, J.; Willis, A. C. *Dalton Trans.* **2009**, 7537.

(27) Sircoglou, M.; Bontemps, S.; Mercy, M.; Saffon, N.; Takahashi, M.; Bouhadir, G.; Maron, L.; Bourissou, D. *Angew. Chem., Int. Ed.* **2007**, *46*, 8583.

(28) Bontemps, S.; Bouhadir, G.; Gu, W.; Mercy, M.; Chin, C.-H.; Foxman, B. M.; Maron, L.; Ozerov, O. V.; Bourissou, D. *Angew. Chem., Int. Ed.* **2008**, *47*, 1481.

(29) Sircoglou, M.; Bontemps, S.; Bouhadir, G.; Saffon, N.; Miqueu, K.; Gu, W.; Mercy, M.; Chen, C.-H.; Foxman, B. M.; Maron, L.; Ozerov, O. V.; Bourissou, D. *J. Am. Chem. Soc.* **2008**, *130*, 16729.

(30) Sircoglou, M.; Mercy, M.; Saffon, N.; Coppel, Y.; Bouhadir, G.; Maron, L.; Bourissou, D. *Angew. Chem., Int. Ed.* **2009**, *48*, 3454.

(31) Derrah, E. J.; Sircoglou, M.; Mercy, M.; Ladeira, S.; Bouhadir, G.; Miqueu, K.; Maron, L.; Bourissou, D. *Organometallics* **2011**, *30*, 657.

(32) Gualco, P.; Lin, T.-P.; Sircoglou, M.; Mercy, M.; Ladeira, S.; Bouhadir, G.; Pérez, L. M.; Amgoune, A.; Maron, L.; Gabbaï, F. P.; Bourissou, D. *Angew. Chem., Int. Ed.* **2009**, *48*, 9892.

(33) Wade, C. R.; Ke, I.-S.; Gabbaï, F. P. *Angew. Chem., Int. Ed.* **2012**, *51*, 478.

(34) Lin, T.-P.; Ke, I.-S.; Gabbaï, F. P. *Angew. Chem., Int. Ed.* **2012**, *51*, 4985.

(35) Tschersich, C.; Limberg, C.; Roggan, S.; Herwig, C.; Ernsting, N.; Kovalenko, S.; Mebs, S. *Angew. Chem., Int. Ed.* **2012**, *51*, 4989.

(36) Bennett, M. A.; Contel, M.; Hockless, D. C. R.; Welling, L. L. *Chem. Commun.* **1998**, 2401.

(37) Bennett, M. A.; Contel, M.; Hockless, D. C. R.; Welling, L. L.; Willis, A. C. *Inorg. Chem.* **2002**, *41*, 844.

(38) Kim, Y.-J.; Kwak, Y.-S.; Joo, Y.-S.; Lee, S.-W. *J. Chem. Soc., Dalton Trans.* **2002**, 144.

(39) Cordero, B.; Gómez, V.; Platero-Prats, A. E.; Revés, M.; Echeverría, J.; Cremades, E.; Barragán, F.; Avarez, S. *Dalton Trans.* **2008**, 2832.

(40) Angermaier, K.; Zeller, E.; Schmidbaur, H. *J. Organomet. Chem.* **1994**, *472*, 371.

(41) Belyakova, O. A.; Slovokhotov, Y. L. *Russ. Chem. Bull.* **2003**, *52*, 1.

(42) Usón, R.; Laguna, A.; Laguna, M. *Inorg. Synth.* **1989**, *26*, 85.

DOI: 10.1021/acs.inorgchem.5b00939
Inorg. Chem. 2015, 54, 6947−6957

(43) Bruce, M. I.; Nicholson, B. K.; bin Shawkataly, O. *Inorg. Synth.* **1989**, *26*, 324.
(44) *SMART ver. 5.625 software for the CCD Detector System*; Bruker AXS Inc.: Madison, WI, 2001.
(45) *SAINTPLUS ver. 6.22 software for the CCD Detector System*; Bruker AXS Inc.: Madison, WI, 2001.
(46) SADABS program for absorption correction using SMART CCD data based on the method of Blessing: Blessing, R. H. *Acta Crystallogr., Sect. A* **1995**, *51*, 33.
(47) Sheldrick, G. M. *SHELXTL*, ver. 6.10; University of Göttingen: Göttingen, Germany, 1994.
(48) Baerends, E. J.; Ziegler, T.; Autschbach, J.; Bashford, D.; Bérces, A.; Bickelhaupt, F. M.; Bo, C.; Boerrigter, P. M.; Cavallo, L.; Chong, D. P.; Deng, L.; Dickson, R. M.; Ellis, D. E.; van Faassen, M.; Fan, L.; Fischer, T. H.; Fonseca Guerra, C.; Ghysels, A.; Giammona, A.; van Gisbergen, S. J. A.; Götz, A. W.; Groeneveld, J. A.; Gritsenko, O. V.; Grüning, M.; Gusarov, S.; Harris, F. E.; van den Hoek, P.; Jacob, C. R.; Jacobsen, H.; Jensen, L.; Kaminski, J. W.; van Kessel, G.; Kootstra, F.; Kovalenko, A.; Krykunov, M. V.; van Lenthe, E.; McCormack, D. A.; Michalak, A.; Mitoraj, M.; Neugebauer, J.; Nicu, V. P.; Noodleman, L.; Osinga, V. P.; Patchkovskii, S.; Philipsen, P. H. T.; Post, D.; Pye, C. C.; Ravenek, W.; Rodríguez, J. I.; Ros, P.; Schipper, P. R. T.; Schreckenbach, G.; Seldenthuis, J. S.; Seth, M.; Snijders, J. G.; Solà, M.; Swart, M.; Swerhone, D.; te Velde, G.; Vernooijs, P.; Versluis, L.; Visscher, L.; Visser, O.; Wang, F.; Wesolowski, T. A.; van Wezenbeek, E. M.; Wiesenekker, G.; Wolff, S. K.; Woo, T. K.; Yakovlev, A. L. ADF2012, SCM, Theoretical Chemistry, Vrije Universiteit, Amsterdam, The Netherlands, http://www.scm.com.
(49) Fonseca Guerra, C.; Snijders, J. G.; te Velde, G.; Baerends, E. J. *Theor. Chem. Acc.* **1998**, *99*, 391.
(50) te Velde, G.; Bickelhaupt, F. M.; Baerends, E. J.; Fonseca Guerra, C.; van Gisbergen, S. J. A.; Snijders, J. G.; Ziegler, T. *J. Comput. Chem.* **2001**, *22*, 931.
(51) Perdew, J. P.; Burke, K.; Ernzerhof, M. *Phys. Rev. Lett.* **1996**, *77*, 3865.
(52) Grimme, S.; Antony, J.; Ehrlich, S.; Krieg, H. *J. Chem. Phys.* **2010**, *132*, 154104.
(53) van Lenthe, E.; Baerends, E. J. *J. Comput. Chem.* **2003**, *24*, 1142.
(54) Harriman, J. E. *Theoretical Foundations of Electron Spin Resonance*; Academic Press: New York, 1978.
(55) Chang, C.; Pelissier, M.; Durand, P. *Phys. Scr.* **1986**, *34*, 394.
(56) Heully, J.-L.; Lindgren, I.; Lindroth, E.; Lundqvist, S.; Mårtensson-Pendrill, A.-M. *J. Phys. B: At. Mol. Phys.* **1986**, *19*, 2799.
(57) van Lenthe, E.; Baerends, E. J.; Snijders, J. G. *J. Chem. Phys.* **1993**, *99*, 4597.
(58) Glendening, E. D.; Badenhoop, J. K.; Reed, A. E.; Carpenter, J. E.; Bohmann, J. A.; Morales, C. M.; Landis, C. R.; Weinhold, F. *NBO 6.0*; Theoretical Chemistry Institute, University of Wisconsin: Madison, WI, 2013, http://nbo6.chem.wisc.edu/.
(59) Becke, A. D.; Edgecombe, K. E. *J. Chem. Phys.* **1990**, *92*, 5397.
(60) Johnson, E. R.; Keinan, S.; Mori-Sánchez, P.; Contreras-García, J.; Cohen, A. J.; Yang, W. *J. Am. Chem. Soc.* **2010**, *132*, 6498.
(61) Becke, A. D. *J. Chem. Phys.* **1993**, *98*, 1372.
(62) Stephens, P. J.; Devlin, F. J.; Chabalowski, C. F.; Frisch, M. J. *J. Phys. Chem.* **1994**, *98*, 11623.

DOI: 10.1021/acs.inorgchem.5b00939
Inorg. Chem. 2015, 54, 6947−6957